



# ECMO implantation training: Needle penetration in 3D printable materials and porcine aorta

Christoph Salewski,<sup>1</sup>  Sebastian Spintzyk,<sup>2</sup> Thore von Steuben,<sup>2</sup> Rodrigo Sandoval Boburg,<sup>1</sup> Attila Nemeth,<sup>1</sup> Christine Schille,<sup>2</sup> Metesh Acharya,<sup>3</sup> Jürgen Geis-Gerstorfer,<sup>2</sup> Hans-Peter Wendel,<sup>1</sup> Aron-Frederik Popov<sup>1</sup> and Christian Schlensak<sup>1</sup>

## Abstract

**Aim** Patients with cardiogenic shock or ARDS, for example, in COVID-19/SARS-CoV-2, may require extracorporeal membrane oxygenation (ECMO). An ECLS/ECMO model simulating challenging vascular anatomy is desirable for cannula insertion training purposes. We assessed the ability of various 3D-printable materials to mimic the penetration properties of human tissue by using porcine aortae.

**Methods:** A test bench for needle penetration and piercing in sampled porcine aorta and preselected 3D-printable polymers was assembled. The 3D-printable materials had Shore A hardness of 10, 20, and 50. 17G Vygon 1.0 × 1.4 mm × 70 mm needles were used for penetration tests.

**Results:** For the porcine tissue and Shore A 10, Shore A 20, and Shore A 50 polymers, penetration forces of 0.9036 N, 0.9725 N, 1.0386 N, and 1.254 N were needed, respectively. For piercing through the porcine tissue and Shore A 10, Shore A 20, and Shore A 50 polymers, forces of 0.8399 N, 1.244 N, 1.475 N, and 1.482 N were needed, respectively. ANOVA showed different variances among the groups, and pairwise two-tailed t-tests showed significantly different needle penetration and piercing forces, except for penetration of Shore A 10 and 20 polymers ( $p = 0.234$  and  $p = 0.0857$ ). Significantly higher forces were required for all other materials.

**Conclusion:** Shore A 10 and 20 polymers have similar needle penetration properties compared to the porcine tissue. Significantly more force is needed to pierce through the material fully. The most similar tested material to porcine aorta for needle penetration and piercing in ECMO-implantation is the silicon Shore A 10 polymer. This silicon could be a 3D-printable material in surgical training for ECMO-implantation.

## Keywords

extracorporeal membrane oxygenation; ECMO; extracorporeal life support; ECLS; COVID-19; SARS-CoV-2; 3D printing; medical education; ZwickRoell; needle penetration

## Introduction

In cardiogenic shock, the limitation in blood circulation throughout the human body may compromise survival. Similarly, pulmonary oxygenation may not be sufficient in patients infected with COVID-19/SARS-CoV-2. The extracorporeal life support system (ECLS) is a miniature heart-lung-machine that can be implanted temporarily through major vessels, for example, via the femoral vessels. In these patients, ECLS could bridge cardiogenic shock. Extracorporeal membrane oxygenation (ECMO) and ECLS both refer to the oxygenation and decarboxylation of blood and its reperfusion into the body. Both support cardiac and/or pulmonary function. ECLS and

ECMO necessitate safe vascular access to the main vessels of the body, such as the femoral artery and the

<sup>1</sup>Department of Thoracic and Cardiovascular Surgery, University Medical Center Tübingen, Tübingen, Germany

<sup>2</sup>Section for Medical Material Science & Technology at the Department of Thoracic and Cardiovascular Surgery, University Medical Center Tübingen, Tübingen, Germany

<sup>3</sup>Department of Cardiac Surgery, Glenfield Hospital, Leicester, UK

### Corresponding author:

Christoph Salewski, Department of Thoracic and Cardiovascular Surgery, University Medical Center Tübingen, Hoppe-Seyler-Strasse 3, Tübingen, 72076, Germany.

Email: [christoph.salewski@uni-tuebingen.de](mailto:christoph.salewski@uni-tuebingen.de)

femoral and/or jugular vein. Vascular access is usually established by direct or ultrasound-guided cannula insertion via the Seldinger technique. In cardiogenic shock, this must be achieved as rapidly as possible. In a resuscitation scenario, the artery may collapse and thus be difficult to locate. Opportunities for cannula insertion in controlled conditions are rare, and an expert must rapidly determine the optimal site of needle insertion. Additionally, anatomical variability and vessel calcification may hinder vascular access, thus highlighting the importance of a dedicated ECMO training model.

An ECLS/ECMO training loop is being developed to simulate cannula insertion in laboratory conditions. After defining a work-flow for 3D printing and adapting vessel geometry to needle insertion difficulty, a 3D-printable material must now be found that mimics large-vessel needle penetration properties. We, therefore, developed a test bench and tested preselected 3D printable polymers against porcine aorta. The aim is to find a 3D-printable material to best mimic human vascular tissue.

## Methods

The test stand was mounted on a Zwick Z010 electric materials testing machine. The upper frame was mobile, and the lower platform served as a socket. A clamp for a 17 G penetration needle was mounted on the top frame. The clamped needle was moved with a velocity of 1 mm/min towards the sample in the lower clamp. The lower frame contained a clamp for the sample material. This clamp was designed to simulate wall tension as induced by the blood pressure within the groin vessels. The sample in the lower clamp was aligned 60° to the vertical axis. The needle would be inserted into the sample at this angle, while the eye of the needle was facing front. Radially the sample was sewn to eight Mersilene 1-0 threads, on which weights symmetrically induced tension. Every 45°, the sample was hooked to another mass. The Laplace pipe formula for wall tension (Formula 1 and 2) returned the individually calculated weights. Axial and tangential tensions were calculated. The transmural wall pressure  $p$  was assumed to be an ideal value of 120 mmHg systolic, which equals 0.0159 N/mm<sup>2</sup>.

$$\sigma_t = \frac{p \cdot d_m}{2 \cdot s}$$

*Formula 1: tangential tension  $\sigma_t$  [N/mm<sup>2</sup>], transmural pressure  $p$  [N], mean diameter of the vessel wall  $d_m$  [mm], wall thickness  $s$  [mm]*

$$\sigma_a = \frac{p \cdot d_m}{4 \cdot s}$$

*Formula 2: axial tension  $\sigma_a$  [N/mm<sup>2</sup>], transmural pressure  $p$  [N], mean diameter of the vessel wall  $d_m$  [mm], wall thickness  $s$  [mm]*

The button-shaped samples with 20 mm diameter had a wall thickness of 2 mm. Porcine aortae and buttons of 3D printable materials were retrieved for the test. The porcine aortae were retrieved from the local abattoir, thus there were no animals harmed for the study. The hearts and aortae were remains of the food production process. No ethical approval was needed. The mediastinal structures containing heart, oesophagus, trachea, and aorta were dissected and the aorta was isolated. The aorta was cut along its long axis so 20 mm full thickness punches could be taken. The aortae had a mean diameter  $d_m$  33 mm for the calculation of wall tension. The area  $A$  [mm<sup>2</sup>] was the cross-sectional area ("edge of the coin") of the sample being the product of the circumference  $c$  [mm] and the wall thickness  $s$  [mm]. The weight at the top 0° and bottom 180° induce axial tension only, whereas the masses at 90° and 270° induce tangential tension only. The four weights at 45°, 135°, 225°, and 315° cause axial and tangential tension of equal amounts. This was respected in their design. Formula 1 returns the tangential tension, and formula 2 returns the axial tension. With formula 3 to formula 6 and  $A_{1/8} = 15.71 \text{ mm}^2$ , the required masses were returned by formula 7.

$$A = c \cdot s$$

*Formula 3: Cross-sectional area  $A$  [mm<sup>2</sup>], circumference  $c$  [mm], wall thickness  $s$  [mm]*

$$F_1 = A_{1/8} \cdot \sigma_a$$

*Formula 4: Force  $F_1$  [N] to induce axial tension, an eighth of the sample area  $A_{1/8}$  [mm<sup>2</sup>], axial tension*

$\sigma_a$  [N/mm<sup>2</sup>].

$$F_2 = A_{1/8} \cdot \sigma_t$$

*Formula 5: Force  $F_2$  [N] to induce tangential tension, an eighth of the sample area  $A_{1/8}$  [mm<sup>2</sup>], tangential*

*tension  $\sigma_t$  [N/mm<sup>2</sup>].*

$$F_3 = A_{1/8} \cdot \left( \frac{\sigma_a + \sigma_t}{2} \right)$$

*Formula 6: Force  $F_3$  [N] to induce axial and tangential tension, an eighth of the sample area  $A_{1/8}$  [mm<sup>2</sup>], axial and tangential tension  $\sigma_a, \sigma_t$  [N/mm<sup>2</sup>].*



**Figure 1.** (Left) Zwick electrical testing machine with sample clamp. (Right) Blue silicone Shore A 10 sample with eight Mersilene 1-0 threads tied 45° apart each. The weights with the masses  $m_1$  pull up and down, the weights with the masses  $m_2$  pull left and right. The weights with the masses  $m_3$  pull in diagonal directions.

$$m_{1,2,3} = \frac{F_{1,2,3}}{g}$$

*Formula 7: Masses  $m_{1,2,3}$  [kg] that induce the axial and radial tension, Forces  $F_{1,2,3}$  [N], acceleration of gravity  $g$  9.81 [m/s<sup>2</sup>]*

The tangential wall tension was calculated as 0.132 N/mm<sup>2</sup> and the axial wall tension as 0.066 N/mm<sup>2</sup>. The button edge area was calculated with 125.66 mm<sup>2</sup>. As there are eight sutures at each sample, the cross-sectional area was evenly distributed by eight. Since  $A1/8 = 15.71$  mm<sup>2</sup>, the axial forces were  $F_1 = 1.03$  N and the tangential forces were  $F_2 = 2.07$  N.  $F_3$  has evenly axial and tangential components and results in  $F_3 = 1.56$  N. Mass  $m_1$  was calculated to be approximately 105 g,  $m_2$  was approximately 211 g, and  $m_3$  was approximately 156 g. The test stand was designed for an inclination of 60° of needle penetration.

The masses were hooked up to the sample by Mersilene 1-0 threads and evenly distributed along the circumference. The two weights with the masses  $m_1$  were allocated at 0° and 180°. The two weights with the masses  $m_2$  were allocated at 90° and 270°. The four weights with the masses  $m_3$  were allocated at 45°, 135°, 225°, and 315°. Frictional forces between the Mersilene threads and the mock loop were neglected. Figure 1 shows the experimental set-up.

Figure 2 shows the stages of needle penetration through the material on the left half. In A and B, the needle is penetrating the material, and piercing through it in C and D. Penetrating results in the peak

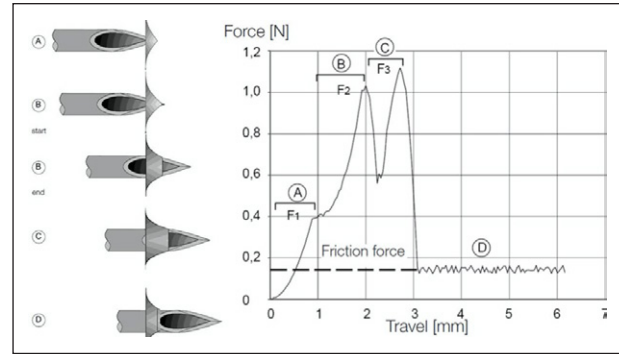


**Figure 2.** (Left) Stage of needle penetration. (Right) Force-travel diagram.

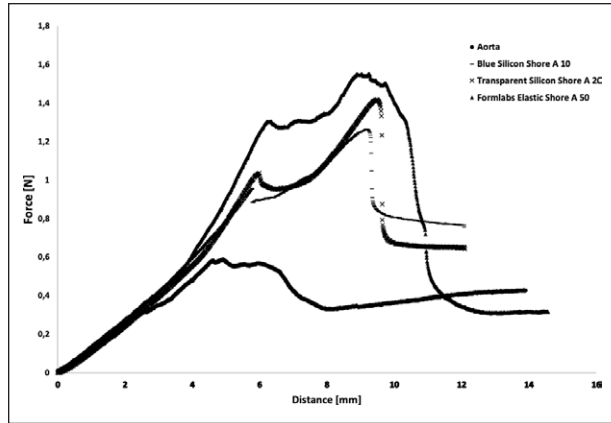
From: ISO 11040-4:2015(en).<sup>1</sup>

$F_2$  on the force-travel diagram, while piercing results in the peak  $F_3$ , as shown on the right side of Figure 2. The needle moved forward at a speed of 1 mm/min and pierced through the probe. A time-force diagram was deduced by the Zwick materials testing machine. The materials assessed were porcine aorta, Silicon blue with a hardness of Shore A 10, Silicon transparent Shore A 20 (both from Silconic® GmbH & Co. KG, Lonsee, Germany), and Formlabs elastic Shore A 50. The porcine samples were taken from the thoracic aorta. All polymers were 3D printable. The Shore A hardness is an industrial standard to describe the hardness of polymers. The higher the value the harder the material. In the Shore A hardness scale, a cone of 1.4 mm is pressed for 15 s into the test sample with 1 kg force. The ratio of the achieved depth of 2.54 mm is scaled from 0 (full distance) to 100 (null distance). For example, Shore A 50 has a penetration in 15 s with 1 kg of 1.27 mm into the test sample. Skin has a hardness value of approx. Shore A 20.

Local maxima for penetration of and piercing through the material were recorded and statistically analysed. An analysis of variance (ANOVA) was conducted with the results for  $F_2$  and  $F_3$  for the four groups of materials. It showed that there was at least one group with different penetration/piercing force than the others. Therefore 6 two-tailed t-tests were calculated comparing each of the three pairs. Aorta vs silicon blue Shore A10, aorta vs silicon transparent Shore A 20, aorta vs Formlabs Elastic Shore A 50, silicon blue Shore A10 vs silicon transparent Shore A 20, silicon blue Shore A 10 vs Formlabs Elastic Shore A 50, Silicon transparent Shore A 20 vs. Formlabs Elastic Shore A 50) This resulted in twelve t-tests.

## Results

The axial forces of the needle penetrating and piercing the material were recorded and plotted in a force-travel



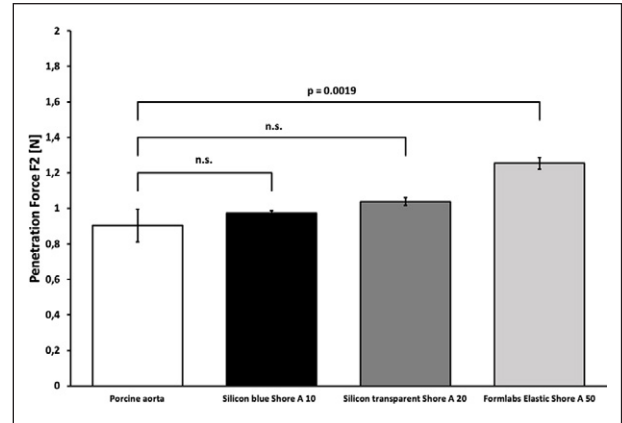
**Figure 3.** Sample course of four graphs of Porcine Aorta, Silicon Shore A 10 and A 20, and Formlabs elastic Shore A 50. There are peaks for maximal penetration force and maximal piercing force in every graph, as in Figure 2.

diagram. The graphs showed two peaks with two subsequent drops of force (Figures 2 and 3). The first drop occurred when the needle tip cut through the material, and less material would resist its progress. Then again, as the broader eye of the needle entered the material, the force to fully pierce the material rose. After the whole diameter of the eye of the needle pierced the material, the force dropped again and formed a slope defined by the friction of the needle shaft only. Friction between the needle shaft and the polymer occurred after penetration and was neglected in this study. The penetration and piercing forces were measured in three dissimilar materials compared to those of a porcine aorta. The materials have different consistencies each, and therefore require varying degrees of force to penetrate and pierce.

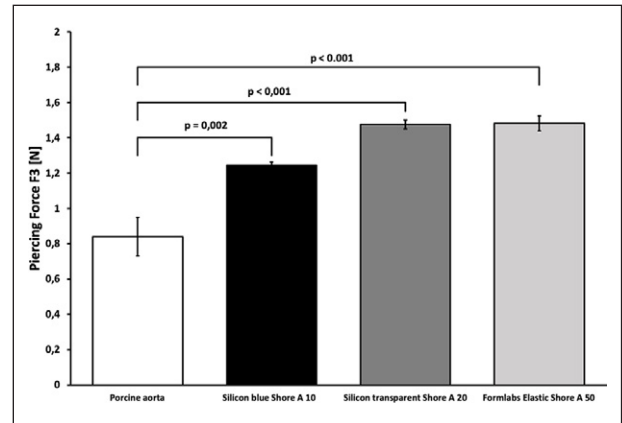
The majority of the t-tests showed significantly different means between groups. However, the force needed to penetrate porcine aorta (0.90 N), silicon blue Shore A 10 (0.97 N), and silicon transparent Shore A 20 (1.03 N) were not significantly different from each other. On the other hand, all groups had significantly different values for piercing force  $F_3$ .

Figure 4 shows the force needed to penetrate each of the materials and a comparison with the porcine aorta. Although the porcine aorta requires the least amount of force to be penetrated when compared to the blue and transparent silicones (Shore A10 and 20), there was no significant difference in the force required to penetrate them. However, the force needed to penetrate the Formlabs Elastic Shore A 50 was significantly higher ( $p=0.0019$ ).

As seen in Figure 5, the porcine aorta required the least amount of piercing force when compared to the other materials. The porcine aorta was associated with a mean piercing force of 0.84 N which is significantly less than the 1.24 N for Silicon blue Shore, and 1.48 N



**Figure 4.** Penetration Force  $F_2$  (Newtons). Error bars depict standard error of means.



**Figure 5.** Piercing Force  $F_3$  (Newtons). Error bars depict standard error of means.

for both Silicon transparent Shore A20 and Formlabs elastic Shore A 50 ( $p$  0.002,  $<0.001$  and  $<0.001$ , respectively). These results suggest that the greater consistency of the synthetic materials do not resemble that of the porcine aorta, making them more difficult to pierce. However, even though being statistically significant, these differences require interpretation. Force needs to be interpreted as the amount of weight that would have to be put on a needle to penetrate and pierce the material. Porcine aorta would need a mean weight of 91.7g to be penetrated (0.90N:  $9.81 \text{ m/s}^2 = 0.0917 \text{ kg} = 91.7 \text{ g}$ ). In comparison, the significantly different Formlabs Elastic needed a mean weight of 127.4 g ( $1.25 \text{ N} : 9.81 \text{ m/s}^2 = 0.1274 \text{ kg} = 127.4 \text{ g}$ ). This is only 35.7 g more than for porcine aorta. On the other hand, silicon blue Shore A 10 needed 99.1 g to be penetrated. ( $0.973 \text{ N} : 9.81 \text{ m/s}^2 = 0.991 \text{ kg} = 99.1 \text{ g}$ ) This is only 7,4 g more than the aorta. 28,3 g ( $127.4 \text{ g} - 91.7 \text{ g}$ ) more weight is needed to penetrate Formlabs Elastic Shore A 50 compared to porcine aorta. The difference



**Figure 6.** Silicon vessel produced from CT data. At the aortic bifurcation, only the right common iliac artery is visible, giving rise to the external iliac artery (lower left corner) and the internal iliac artery (upper left corner). This model is made from two-component dental cast silicon and is not 3D-printed.

is statistically significant, but the relevance for manual needle introduction is questionable. However, silicon blue Shore A 10 (7.4 g) and silicon transparent Shore A20 (13.3 g) show irrelevant higher penetration forces than the porcine aorta. However, in respect of piercing the material, the closest is silicone blue Shore A 10 with 41.2 g more needed than for the aorta, representing a perhaps palpable difference.

## Discussion

Silicon has been used for mimicking tissue properties for needle penetration.<sup>2</sup> However, to produce complex geometry, a 3D printable silicone with exact vessel-like properties has not yet been reported to our knowledge. Needle penetration has been widely investigated, and industrial standards exist.<sup>1</sup> Furthermore, needle penetration tests for biological tissues have been conducted.<sup>3,4</sup> Shore A hardness of porcine aorta has been reported to vary from 12 to 17 Shore A by Riedle et al.<sup>5</sup> Therefore, our test samples fall into the range of the known hardness values. Among the sparse 3D printable polymers with Shore A hardness in the range of tissue, we tested two silicones and one elastic polymer. A two-component dental silicon vessel cast has been produced with remarkable effort, as shown in Figure 6. A 3D printable silicon for this purpose is desirable. Blue Shore A 10 and transparent Shore A 20 silicon show similar needle penetration properties compared to the porcine aorta, whereas none of the tested materials showed identical piercing properties. Every material was more resistant to piercing than aorta itself. Even though 3D printable silicone polymers are flexible and comparable in penetration force, they could be applied with some limitations in ECMO implantation training. Further research

needs to be done to determine other artificial materials with similar needle penetration properties to the aorta.

Other models are available for the teaching and rehearsing of TAVR and EVAR. However, this model focusses on the needle insertion and penetration of vessels, if needed under resuscitation circumstances. Both therapies are not appropriate under resuscitation. So our model focusses on vascular access, only.

Among the three tested 3D printable polymer materials, two Silicon blue Shore A10 and Silicon transparent Shore A20 show similar needle penetration properties compared to porcine aorta. In piercing force, every artificial material needed more force to be pierced completely compared to porcine aorta.

## Acknowledgements

We thank Thore von Steuben for the concept of the excellent needle penetration test stand. Furthermore, we thank Prof. Geis-Gerstorfer for lab resources and Christine Schille for the help in conducting the tests and sampling the data. Rodrigo Sandoval Boburg helped with the manuscript, and we thank Sebastian Spintzyk for preselecting 3D printable silicones and contributing his profound 3D printing knowledge.


## Declaration of Conflicting Interests

The author(s) declared no potential conflicts of interest with respect to the research, authorship, and/or publication of this article.

## Funding

The author(s) received no financial support for the research, authorship, and/or publication of this article.

## ORCID iD

Christoph Salewski  <https://orcid.org/0000-0001-7155-6039>

## References

1. ISO 11040-4:2015(en) Prefilled syringes - Part 4: Glass barrels for injectables and sterilised subassembled syringes ready for filling.
2. Wang Y, Tai BL, Yu H, et al. Silicone-based tissue-mimicking phantom for needle insertion simulation. *J Med Device* 2014; 8: 51.
3. Jiang S, Li P, Yu Y, et al. Experimental study of needle-tissue interaction forces: effect of needle geometries, insertion methods and tissue characteristics. *J Biomech* 2014; 47: 3344–3353.
4. Bao X, Li W, Lu M, et al. Experiment study on puncture force between MIS suture needle and soft tissue. *Biosurf Biotribol* 2016; 2: 49–58.
5. Riedle H, Mukai B, Molz P, et al. Determination of the mechanical properties of aortic tissue for 3D printed surgical models. In: *2018 11th biomedical engineering international conference (BMEiCON)*, Chiang Mai, 21–24 November 2018, pp.1–5. Piscataway, NJ: IEEE.